LETTERS

Allosteric modulation of the presynaptic Ca^{2+} sensor for vesicle fusion

Xuelin Lou[1], Volker Scheuss[1]† & Ralf Schneggenburger[1]

Neurotransmitter release is triggered by an increase in the cytosolic Ca^{2+} concentration ([Ca^{2+}]$_i$), but it is unknown whether the Ca^{2+}-sensitivity of vesicle fusion is modulated during synaptic plasticity. We investigated whether the potentiation of neurotransmitter release by phorbol esters[1–3], which target presynaptic protein kinase C (PKC)/munc-13 signalling cascades[4–6], exerts a direct effect on the Ca^{2+}-sensitivity of vesicle fusion. Using direct presynaptic Ca^{2+}-manipulation and Ca^{2+} uncaging at a giant presynaptic terminal, the calyx of Held, we show that phorbol esters potentiate transmitter release by increasing the apparent Ca^{2+}-sensitivity of vesicle fusion. Phorbol esters potentiate Ca^{2+}-evoked release as well as the spontaneous release rate. We explain both effects by an increased fusion 'willingness' in a new allosteric model of Ca^{2+}-activation of vesicle fusion. In agreement with an allosteric mechanism, we observe that the classically high Ca^{2+} cooperativity in triggering vesicle fusion (~4) is gradually reduced below 3 µM [Ca^{2+}]$_i$, reaching a value of <1 at basal [Ca^{2+}]$_i$. Our data indicate that spontaneous transmitter release close to resting [Ca^{2+}]$_i$ is a consequence of an intrinsic property of the molecular machinery[7,8] that mediates synaptic vesicle fusion.
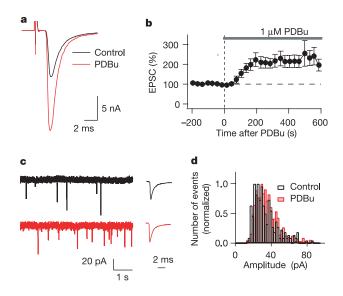
We studied transmitter release modulation at the calyx of Held, a large excitatory synapse of the central nervous system (CNS) that is uniquely accessible to manipulations of the presynaptic intracellular Ca^{2+} concentration[9–11]. Bath application of the phorbol ester phorbol-12,13-dibutyrate (PDBu; 1 µM) led to a potentiation of evoked excitatory postsynaptic currents (EPSCs), which reached a near-maximal value of 227 ± 14% (mean ± s.e.m.) of control after 200 s (Fig. 1a, b). PDBu also increased the frequency of spontaneous, miniature EPSCs (mEPSCs; Fig. 1c), from 1.27 ± 0.3 Hz for control to 5.1 ± 2.1 Hz following bath-application of PDBu. The mean mEPSC amplitudes were unchanged (Fig. 1c, d), indicating that PDBu potentiates synaptic transmission by means of a presynaptic mechanism[4].

To investigate directly whether PDBu potentiates transmitter release by increasing the Ca^{2+}-sensitivity of vesicle fusion[3,12], we made simultaneous pre- and postsynaptic whole-cell recordings, and evoked transmitter release by presynaptic Ca^{2+} uncaging (Fig. 2). Under these conditions of presynaptic whole-cell recordings, the potentiation of EPSCs by PDBu was transient (see Supplementary Fig. 1), an effect that we attribute to the loss of presynaptic signalling molecules and/or the loss of glutamate from the presynaptic terminal[13]. In the experiments shown below, we therefore restricted the analysis to times around the peak of the PDBu-induced potentiation.

EPSCs evoked by weak Ca^{2+} uncaging stimuli, which elevated the presynaptic [Ca^{2+}]$_i$ to 2.5–5 µM, were strongly potentiated by 1 µM PDBu (Fig. 2a). We deconvolved the EPSCs with the estimated mEPSC waveform to derive the transmitter release rates (Fig. 2a; see Methods). The release rate traces in the example shown in Fig. 2a (bottom panel) indicate that transmitter release was potentiated

2.6-fold. On average, we observed a 4.4 ± 1.04-fold potentiation of peak transmitter release rates for flashes that elevated [Ca^{2+}]$_i$ to 2.5–5 µM (n = 6 cells). The integrated transmitter release rate traces (Fig. 2b) could often be separated into a fast and a slow component of release, on the basis of double-exponential fits. In those cells in which the separation was feasible at low [Ca^{2+}]$_i$ (2.5–5 µM; n = 3 out of 6 cells), the amplitude of both the fast and the slow component of release was increased to 288 ± 57% and 432 ± 117% of control, respectively.

When transmitter release was evoked by stronger Ca^{2+}-uncaging stimuli that elevated presynaptic [Ca^{2+}]$_i$ to 10–13 µM, we found that PDBu did not notably potentiate the EPSC amplitudes (Fig. 2c). With these stronger [Ca^{2+}]$_i$ stimuli, the EPSC rose rapidly and had large amplitudes, indicative of the rapid release of a large number of readily releasable vesicles. Application of 1 µM PDBu did not lead to a significant increase in EPSC amplitude or peak transmitter release rates under these conditions (Fig. 2c). However, the rise times of

Figure 1 | Potentiation of evoked EPSCs and miniature EPSC frequency by the phorbol ester PDBu. a, Evoked EPSCs before (black trace), and after (red trace) bath application of 1 µM PDBu. **b**, Average time course of EPSC potentiation by PDBu (mean ± s.e.m; n = 4 cells). **c**, Postsynaptic current before and after application of PDBu. Note that the frequency of mEPSCs increased, but mEPSC amplitude (average traces shown on the right) was virtually unchanged. **d**, mEPSC amplitude histogram before (black) and after (red) application of PDBu. The average mEPSC amplitude was 36.1 pA for control conditions and 38.4 pA after PDBu application. Data shown in **a**, **c** and **d** are from the same cell.

[1]AG Synaptische Dynamik und Modulation und Abt. Membranbiophysik, Max-Planck-Institut für biophysikalische Chemie, Am Fassberg 11, D-37077 Göttingen, Germany.
†Present address: Cold Spring Harbor Laboratory, 1 Bungtown Road, Cold Spring Harbor, New York 11724, USA.

EPSCs were shortened by PDBu application (Fig. 2c, inset), indicating that PDBu slightly speeds up the release process. As $[Ca^{2+}]_i$ steps to 10 μM or more rapidly deplete a pool of readily releasable vesicles[10], the small effect of PDBu on EPSCs evoked by strong Ca^{2+}-uncaging stimuli indicates that PDBu does not induce a marked increase in the pool size. With pool-depleting $[Ca^{2+}]_i$ steps
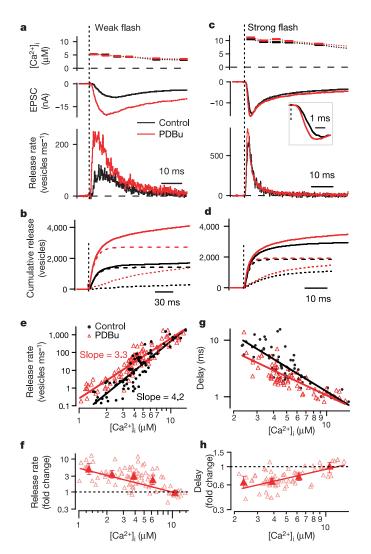
to 10–13 μM, neither the fast nor the slow component of transmitter release was significantly increased by PDBu (Fig. 2d; 102 ± 5% and 105 ± 10% of control, respectively; $n = 7$ pairs each; $P > 0.5$). Similar results were obtained by analysing the cumulative transmitter release rates evoked by pool-depleting presynaptic depolarizations (see Supplementary Fig. 2). These findings indicate that in the calyx of Held, unlike in chromaffin cells[14] and hippocampal neurons[15], PDBu does not significantly increase the size of a readily releasable vesicle pool. Furthermore, PDBu does not change the relative weighting of a rapidly releasable, and a more slowly releasable sub-pool of readily releasable vesicles[16].

Figure 2e summarizes the experiments shown in Fig. 2a–d by plotting the transmitter release rates as a function of $[Ca^{2+}]_i$, both for the control conditions and after applying 1 μM PDBu. The control data (Fig. 2e, black circles, $n = 23$ cell pairs) has a slope of 4.2 ± 0.5 (slope ± 95% confidence interval), as revealed by linear regression after logarithmic transformation of the data set. Conversely, the data obtained in the presence of PDBu (open triangles) has a slope of 3.3 ± 0.3, indicating that PDBu reduces the effective cooperativity with which Ca^{2+} induces vesicle fusion. Figure 2f shows the effect of PDBu relative to the line fitted to the control data in each cell (see Methods). For small $[Ca^{2+}]_i$ steps (up to 1–3 μM), PDBu causes a 4–5-fold increase in release rate ($P < 0.001$; one-sample t-test). The
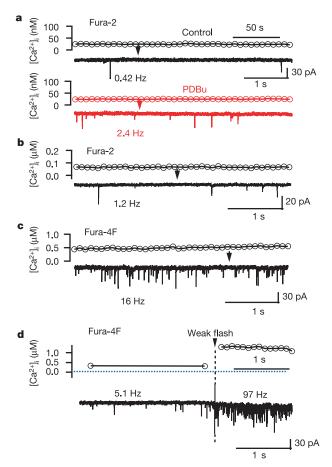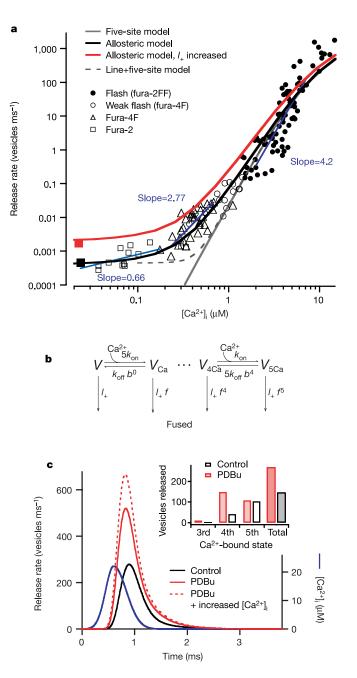

Figure 2 | Presynaptic Ca²⁺ uncaging shows that phorbol ester increases the Ca²⁺ sensitivity of vesicle fusion, concomitant with a reduced Ca²⁺ cooperativity of vesicle fusion. a, Responses to a weak Ca²⁺-uncaging stimulus. The upper, middle and lower panels show presynaptic $[Ca^{2+}]_i$, EPSCs and transmitter release rate, respectively. b, Integrated transmitter release rate traces for the responses in a. The fast (dashed lines) and slow (dotted lines) components of release are shown. c, Same as a, but for a strong Ca²⁺-uncaging stimulus in a different cell pair. The inset shows the EPSC on an expanded time scale. d, Same as b, but for the responses shown in c. In a–d, control responses are shown in black and responses around the peak of the PDBu-potentiation are shown in red. e, Double-logarithmic plot of peak transmitter release rates (as measured in a and c) as a function of presynaptic $[Ca^{2+}]_i$. Lines in e–h are linear regression fits to the logarithmically transformed data sets ($n = 23$ cell pairs). f, Potentiation of peak release rates by PDBu, relative to the fitted line of the control data points in each cell (see Methods). Here (and in h) the individual data points (open symbols) were grouped and averaged (filled symbols), with error bars representing the 95% confidence interval. All groups were significantly different from 1 ($P < 0.003$; one-sample t-test), except for the data at the highest $[Ca^{2+}]_i$ ($P \sim 0.5$) in each plot. g, Synaptic delays as a function of $[Ca^{2+}]_i$, both under control conditions (black) and in the presence of 1 μM PDBu (red). h, Relative change in synaptic delays induced by 1 μM PDBu.

Figure 3 | Transmitter release regulation by presynaptic [Ca²⁺]ᵢ close to resting values. a, Presynaptic $[Ca^{2+}]_i$ (upper trace) and postsynaptic current (lower trace). The presynaptic calyx was pre-loaded with the Ca²⁺-indicator fura-2. The time scale on the $[Ca^{2+}]_i$ trace applies to a–c, and the arrows indicate the times corresponding to the current traces in the lower panels. b, Presynaptic $[Ca^{2+}]_i$ (upper trace) and postsynaptic current (lower trace) in a recording in which the calyx was loaded with a solution containing 100 nM free $[Ca^{2+}]$. c, Same as in b, but for a calyx loaded with 500 nM $[Ca^{2+}]$. d, Presynaptic $[Ca^{2+}]_i$ and postsynaptic current before and after a weak Ca²⁺-uncaging stimulus.

relative effectiveness of PDBu decreases with increasing $[Ca^{2+}]_i$. With $[Ca^{2+}]_i$ steps to $\sim 10\,\mu M$, PDBu does not induce a significant potentiation of peak transmitter release rates (Fig. 2f, rightmost average data point; $P > 0.5$), consistent with the example experiment shown in Fig. 2c. The delay in transmitter release is shortened by PDBu for $[Ca^{2+}]_i$ steps below $8\,\mu M$ (Fig. 2h; $P < 0.003$), indicating that phorbol esters slightly increase transmitter release kinetics.

The results in Fig. 2 show that PDBu increases the intracellular Ca^{2+}-sensitivity of vesicle fusion in response to submaximal Ca^{2+} stimuli. To investigate whether this increase in Ca^{2+}-sensitivity is related to the potentiation of spontaneous transmitter release by phorbol esters[2,4] (Fig. 1c), we related the mEPSC frequency measured in postsynaptic recordings to the $[Ca^{2+}]_i$ in the presynaptic terminal. In a first series of experiments (Fig. 3a), we monitored basal presynaptic $[Ca^{2+}]_i$ after pre-loading calyces with the Ca^{2+} indicator fura-2 during a brief (~ 1–2 min) presynaptic whole-cell recording. PDBu increased the frequency of spontaneous mEPSCs from 0.45 ± 0.05 Hz to 1.7 ± 0.3 Hz ($n = 5$ cells), without a significant

change in the basal $[Ca^{2+}]_i$ (from 24 ± 1 nM to 22 ± 1 nM; Fig. 4a, black and red filled squares). The frequency of unstimulated mEPSCs in these recordings was identical to that observed in experiments without any presynaptic recording (0.41 ± 0.10 Hz; $n = 7$ cells; $P = 0.74$, unpaired t-test). In another series of experiments (Fig. 3b, c), presynaptic $[Ca^{2+}]_i$ was clamped to values higher than baseline, by using strongly Ca^{2+}-buffered presynaptic pipette solutions in simultaneous pre- and postsynaptic recordings. A fluorescent Ca^{2+} indicator (fura-2 or fura-4F; $100\,\mu M$) measured the effective $[Ca^{2+}]_i$ inside the terminal (see Methods). In the example shown in Fig. 3b, presynaptic $[Ca^{2+}]_i$ was ~ 80 nM, and the rate of transmitter release was 1.2 Hz. In the experiment shown in Fig. 3c, $[Ca^{2+}]_i$ was 500 nM, and the average release activity was much higher (16 Hz). In an additional series of experiments, we applied weak Ca^{2+}-uncaging stimuli that elevated presynaptic $[Ca^{2+}]_i$ to 0.3–1.5 μM, and measured the resulting Ca^{2+}-triggered increase in mEPSC frequency (Fig. 3d).

The experiments in Fig. 3 reveal a surprisingly low cooperativity of Ca^{2+} in triggering vesicle release at low $[Ca^{2+}]_i$. We plotted the rates of transmitter release estimated at low $[Ca^{2+}]_i$ (Fig. 3) as a function of $[Ca^{2+}]_i$ (Fig. 4a, squares and open symbols), and also added the data points obtained under control conditions with Ca^{2+} uncaging resulting in higher $[Ca^{2+}]_i$ (Fig. 4a, filled circles). In the double-logarithmic coordinates of this plot, it can be seen that the slope, which corresponds to the exponent in the power relationship between transmitter release and $[Ca^{2+}]_i$, is high at 2–8 μM $[Ca^{2+}]_i$ (slope = 4.2) but becomes progressively smaller at lower $[Ca^{2+}]_i$ (slope = 2.77 at 200–700 nM $[Ca^{2+}]_i$ and slope = 0.66 at 20–200 nM $[Ca^{2+}]_i$; see blue lines in Fig. 4a).

The observed gradual decrease in Ca^{2+} cooperativity at lower $[Ca^{2+}]_i$ does not agree with predictions from conventional models of Ca^{2+}-activation of vesicle fusion, which assume that vesicle fusion occurs exclusively from a fully occupied Ca^{2+}-sensor[9,10]. As expected, the prediction of one such model[10] approached its highest slope at low $[Ca^{2+}]_i$, and predicted basal vesicle fusion rates several orders of magnitude lower than the observed ones (Fig. 4a, continuous grey line). We next tested whether the overall Ca^{2+}-dependency of release could be explained by the sum of a steeply Ca^{2+}-dependent release mechanism and Ca^{2+}-independent, spontaneous release, possibly mediated by molecularly different forms of SNARE (soluble NSF-attachment protein receptor) proteins[17–19]. We therefore added a constant, Ca^{2+}-independent release rate of $0.45\,s^{-1}$ to the prediction

Figure 4 | An allosteric model of Ca^{2+} activation of vesicle fusion. This model explains the Ca^{2+}-sensitivity of transmitter release over a wide range of $[Ca^{2+}]_i$, and explains the effects of PDBu on spontaneous and Ca^{2+}-evoked transmitter release. a, Transmitter release rate as a function of $[Ca^{2+}]_i$. The filled squares are average mEPSC frequency under control conditions (black) and after application of PDBu (red) at basal $[Ca^{2+}]_i$ (see Fig. 3a). Data obtained in Ca^{2+} perfusion experiments (open squares, open triangles; Fig. 3b, c) or with weak Ca^{2+} uncaging (open circles; Fig. 3d) are shown. Control condition data points (closed circles) are re-plotted from Fig. 2e. Lines fitted to the logarithmically transformed data and the resulting slopes are shown in blue. The grey line is the prediction of a five-site model for Ca^{2+}-binding and vesicle fusion, with parameters as in ref. 10. The grey dashed line is the prediction of the five-site model to which a Ca^{2+}-independent release rate of $0.45\,s^{-1}$ was added. The black and red lines are predictions of a simplified allosteric model (b) for two different vesicle fusion rates l_+ (see Methods). c, Transmitter release rates predicted by the allosteric model in response to a brief $[Ca^{2+}]_i$ spike (blue trace). Responses for the standard set of parameters (black trace; see Methods) and for a fivefold increase in vesicle fusion rate l_+ (red trace) are shown. The dashed red trace was obtained by further increasing the $[Ca^{2+}]_i$ transient to 110% of the control value, thus accounting for a 10% increase in presynaptic Ca^{2+} current. The inset shows the absolute number of vesicles released from the third, fourth and fifth Ca^{2+}-bound state (see b), both under control conditions (black) and with a fivefold increase in vesicle fusion rate (l_+).

of the conventional five-site model, resulting in the dashed grey line (Fig. 4a). This prediction markedly underestimates release rates at 200–800 nM $[Ca^{2+}]_i$, where the observed rates were 9.6 ± 0.9-fold higher than the prediction ($n = 46$; $P < 0.001$; one-sample t-test). Finally, the data cannot be explained by a highly Ca^{2+}-sensitive sub-pool of vesicles, as observed in chromaffin cells[20]. This is because the increase in mEPSC frequency in response to a sustained $[Ca^{2+}]_i$ elevation by weak Ca^{2+} uncaging (Fig. 3d) did not show signs of exhaustion, as would be expected for a separate sub-pool of vesicles. Also, adding a single additional sub-pool of vesicles would not explain the rather continuous decrease in Ca^{2+} cooperativity observed below $3\,\mu M$ $[Ca^{2+}]_i$ (Fig. 4a).

The reduction in Ca^{2+} cooperativity at lower $[Ca^{2+}]_i$ is an expected property of allosteric models, which predict conformational changes of biological molecules in the absence of ligand binding[21,22]. Allosteric models might also explain how phorbol esters increase the effective Ca^{2+}-sensitivity of vesicle fusion (Fig. 2). We therefore developed an allosteric model of Ca^{2+}-activated vesicle fusion (Fig. 4b), which allows low rates of vesicle fusion in the absence of bound Ca^{2+} (rate constant, $l_+ = 2 \times 10^{-4}\,s^{-1}$), and in which increasingly higher rates of vesicle fusion are attained when the Ca^{2+}-sensor is more completely occupied (Fig. 4b). This model predicts the rates of transmitter release over the entire range of $[Ca^{2+}]_i$ studied here, from $\sim 25\,nM$ to more than $10\,\mu M$ $[Ca^{2+}]_i$ (Fig. 4a, black line; see Methods for model parameters). The model also accounts for the phorbol-ester-induced potentiation of transmitter release. Assuming that phorbol ester increases the basal fusion 'willingness' (rate constant l_+ in Fig. 4b), an increase in transmitter release at low $[Ca^{2+}]_i$ is predicted (Fig. 4a, compare red and black lines). The increase in l_+ also predicts enhanced fusion rates at intermediate $[Ca^{2+}]_i$ (2–8 μM; Fig. 4a, red line), with decreased effectiveness of PDBu potentiation at higher $[Ca^{2+}]_i$; again, this is as we observed (Fig. 2e, f). Finally, the model predicts the potentiation of transmitter release evoked by a presynaptic action potential (Fig. 4c). In this simulation, the release response to a brief $[Ca^{2+}]_i$ transient (Fig. 4c, blue trace) was modelled[9,10], either for the basal conditions or for a fivefold enhanced rate constant l_+ (Fig. 4c, black and red traces). Taking into account an $\sim 10\%$ increase in presynaptic Ca^{2+} current by PDBu (see Supplementary Fig. 2), a potentiation of transmitter release to 228% of control is predicted (compare the black and the dotted red trace in Fig. 4c), similar as observed for EPSCs evoked by afferent fibre stimulation ($227 \pm 14\%$, Fig. 1b). The model predicts that the potentiation of transmitter release in response to a presynaptic action potential is largely due to increased release out of the fourth Ca^{2+}-bound state, whereas release out of the fully Ca^{2+}-bound state is unaffected (see Fig. 4c, inset).

We have shown that phorbol esters increase transmitter release by enhancing the Ca^{2+}-sensitivity of vesicle fusion, without a significant increase in the size of the readily releasable vesicle pool (Fig. 2d and Supplementary Fig. 2), but with a small contribution from an enhanced presynaptic Ca^{2+} current (see Supplementary Fig. 2). In pituitary cells, phorbol esters increase Ca^{2+}-sensitivity by increasing the vesicle pool depletion time constants[23]; however, such an increase is not apparent at the calyx of Held (Fig. 2b). In the framework of a simple allosteric model, phorbol esters enhance the apparent Ca^{2+}-sensitivity by increasing the 'willingness' of vesicle fusion, corresponding to an increase in the rate constant l_+ (Fig. 4b), without a change in the Ca^{2+}-binding properties of the Ca^{2+}-sensor for vesicle fusion. An increased fusion willingness might be caused by lowering the energy barrier for vesicle fusion, a mechanism also implicated in short-term synaptic enhancement and in Ca^{2+}-independent, hypertonicity-evoked transmitter release[24]. Our allosteric model predicts that an enhanced fusion willingness potentiates the rate of vesicle fusion at baseline $[Ca^{2+}]_i$, as well as the rate of Ca^{2+}-evoked vesicle fusion in an intermediate range of $[Ca^{2+}]_i$ (Fig. 4a, c). Our observations thus explain the link between an increase in the rate of unstimulated transmitter release and a

concomitant increase in transmitter release probability, observed during many forms of presynaptic plasticity[2,25,26].

Synaptic vesicle fusion at resting $[Ca^{2+}]_i$ does not appear to be constitutive. Rather, it is regulated by phorbol esters as well as by Ca^{2+} (Fig. 3), although the Ca^{2+} cooperativity is low close to baseline $[Ca^{2+}]_i$ (<1; Fig. 4a). Evidence for a low Ca^{2+} cooperativity close to resting $[Ca^{2+}]_i$ has also been obtained at neuromuscular synapses[27,28]. This low Ca^{2+} cooperativity is functionally relevant, because it prevents a large increase in asynchronous release activity during moderate elevations of residual $[Ca^{2+}]_i$, which would be expected if a steeply Ca^{2+}-dependent mechanism operated close to baseline $[Ca^{2+}]_i$. It has been shown that genetic deletion of the SNARE proteins synaptobrevin[17,18] or SNAP-25 (ref. 19) affect Ca^{2+}-evoked release more strongly than unstimulated release or release stimulated by hypertonicity. This is consistent with our observations, if our simplified allosteric model is assumed to describe the kinetic responses of a complex of several proteins (including SNAREs and synaptotagmins) in synaptic vesicle fusion[7,8]. Removing one essential protein might affect the increase in vesicle fusion rate upon Ca^{2+}-binding (rate constant f in Fig. 4b) to a greater degree than the basal fusion 'willingness' (rate constant l_+ in Fig. 4b). In our view, spontaneous and Ca^{2+}-evoked transmitter release thus emerge from a fine-tuned molecular complex that mediates vesicle fusion at synapses.

METHODS

Slice preparation and electrophysiology. Transverse brainstem slices (200 μm) containing the medial nucleus of the trapezoid body (MNTB) were prepared from 8–11-day-old rat brains using a vibratome. Simultaneous whole-cell patch-clamp recordings from a postsynaptic MNTB principal cell and its presynaptic calyx of Held were made under visual control, using an EPC10/2 double amplifier (HEKA). Both cells were voltage-clamped at $-80\,mV$, and series resistance was compensated up to 90%. The remaining error in the postsynaptic currents was corrected off-line. The extracellular solution was a bicarbonate buffered Ringer solution (for example, see ref. 11) with 2 mM $CaCl_2$ and 1 mM $MgCl_2$. For paired recordings, $0.5\,\mu M$ tetrodotoxin, 10 mM tetraethylammonium chloride (TEA), $50\,\mu M$ D-2-amino-5-phosphonovaleric acid and $100\,\mu M$ cyclothiazide (CTZ) were added to the solution. For experiments with strong Ca^{2+}-uncaging stimuli (Fig. 2c, d), 2 mM γ-D-glutamyl-glycine (γ-DGG) was also present to prevent AMPA-receptor saturation. The pipette (intracellular) solution contained caesium-gluconate[11], with 0.2 and 5 mM EGTA for pre- and postsynaptic recordings, respectively. Experiments were done at room temperature (21–24 °C). In some experiments, EPSCs were evoked by afferent fibre stimulation without simultaneous presynaptic recording (Fig. 1).

Ca^{2+} uncaging and Ca^{2+} imaging. For Ca^{2+} uncaging, the presynaptic pipette (intracellular) solution contained (mM): 130 caesium gluconate, 20 TEA-Cl, 20 HEPES, 5 Na_2ATP, 0.3 Na_2GTP, 0.1 fura-2FF (Teflabs), 1 DM-nitrophen (Calbiochem), 0.85 $CaCl_2$ and 0.5 $MgCl_2$. Ca^{2+} uncaging was done with a flash lamp (Rapp Optoelektronik), and $[Ca^{2+}]_i$ was measured by imaging the fluorescence of fura-2FF with a slow-scan CCD camera (TILL-photonics) at excitation wavelengths of 350 and 380 nm. $[Ca^{2+}]_i$ was calculated from background-corrected fluorescence ratios, using calibration procedures as described[11].

For clamping the presynaptic $[Ca^{2+}]_i$ in the range of 0.05–1 μM (Fig. 3b, c), the presynaptic pipette solution contained 20 mM EGTA, to which different concentrations of $CaCl_2$ were added to yield nominal free $[Ca^{2+}]$ of 50, 100, 300 and 600 nM. The effective presynaptic $[Ca^{2+}]_i$ was measured with fura-2 or fura-4F added to the intracellular solution (100 μM).

Data analysis and simulations. Analysis routines were written in IgorPro (Wavemetrics). Miniature EPSCs were detected using a template matching routine. Transmitter release rates were calculated by deconvolving the measured EPSCs with an idealized mEPSC waveform with double-exponential decay[10,16]. The deconvolution assumes that EPSCs arise from linearly summed mEPSCs with amplitudes of 30 pA (for CTZ) and 15 pA (for CTZ and γ-DGG), and an additional current component generated by glutamate spillover, which was subtracted. The minimal synaptic delays (Fig. 2g) are expressed as the time between the trigger of the flash lamp and the occurrence of five quanta in integrated release-rate traces. Cumulative release rates were fitted with double-exponential functions. An exponential with the fitted parameters for the fast component (dashed lines in Fig. 2b, d) was subtracted from the data trace to yield the isolated slow component (dotted lines in Fig. 2b, d). Unless stated

otherwise, data are reported as mean $\pm$ s.e.m., and statistical significance was determined by paired t-tests.

The relative change in transmitter release rates induced by PDBu (Fig. 2f) was calculated for individual cells as follows[11]. First, the line fit to the logarithmically-transformed control data set (Fig. 2e, black line) was shifted on the x axis (log ($[Ca^{2+}]_i$)) to fit the control data points for a given recording. Then, the difference in y value (log (release rate)) between each data point obtained in PDBu and the shifted fit line was read out. In this way, possible differences in $[Ca^{2+}]_i$ are taken into account. The relative change in delays (Fig. 2h) was analysed in the same way.

Ca^{2+}-dependent vesicle fusion rates were simulated using a conventional five-site model[10] and a simplified allosteric model (Fig. 4b). Both models were solved numerically. Release was assumed to occur from a homogeneous pool of 2,000 vesicles. The simulations according to the five-site model (Fig. 4a, continuous grey line) were made with the parameters given in ref. 10. Parameter values for the simplified allosteric model (Fig. 4b) were constrained as follows. First, the factor determining the increase in vesicle fusion rate upon Ca^{2+}-binding, f, was set to 31.3, giving $l_+ \times f^5 = 6,000\,s^{-1}$, identical to the fusion rate (γ) of the five-site model in ref. 10. Then, k_{on} ($1 \times 10^8\,M^{-1}\,s^{-1}$), k_{off} ($4,000\,s^{-1}$) and the cooperativity factor, b (0.5) were set such that the predictions of the two models at $[Ca^{2+}]_i > 7\,\mu M$ were similar (Fig. 4a). Finally, the rate constant $l_+ (2 \times 10^{-4}\,s^{-1})$ was set to fit the vesicle fusion rate at low $[Ca^{2+}]_i$. For predicting release in the presence of phorbol ester (red traces in Fig. 4a, c), l_+ was increased fivefold, with all other parameters unchanged.

1. Malenka, R. C., Madison, D. V. & Nicoll, R. A. Potentiation of synaptic transmission in the hippocampus by phorbol ester. *Nature* **321**, 175–177 (1986).
2. Shapira, R., Silberberg, S. D., Ginsburg, S. & Rahamimoff, R. Activation of protein kinase C augments evoked transmitter release. *Nature* **325**, 58–60 (1987).
3. Yawo, H. Protein kinase C potentiates transmitter release from the chick ciliary presynaptic terminal by increasing the exocytotic fusion probability. *J. Physiol. (Lond.)* **515**, 169–180 (1999).
4. Hori, T., Takai, Y. & Takahashi, T. Presynaptic mechanism for phorbol ester-induced synaptic potentiation. *J. Neurosci.* **19**, 7262–7267 (1999).
5. Rhee, J.-S. *et al.* β phorbol ester- and diacylglycerol-induced augmentation of transmitter release is mediated by munc13s and not by PKCs. *Cell* **108**, 121–133 (2002).
6. Silinsky, E. M. & Searl, T. J. Phorbol esters and neurotransmitter release: More than just protein kinase C? *Br. J. Pharmacol.* **138**, 1191–1201 (2003).
7. Chen, Y. A. & Scheller, R. H. SNARE-mediated membrane fusion. *Nature Rev. Mol. Cell Biol.* **2**, 98–106 (2001).
8. Jahn, R., Lang, T. & Südhof, T. C. Membrane fusion. *Cell* **112**, 519–533 (2003).
9. Bollmann, J., Sakmann, B. & Borst, J. Calcium sensitivity of glutamate release in a calyx-type terminal. *Science* **289**, 953–957 (2000).
10. Schneggenburger, R. & Neher, E. Intracellular calcium dependence of transmitter release rates at a fast central synapse. *Nature* **406**, 889–893 (2000).
11. Felmy, F., Neher, E. & Schneggenburger, R. Probing the intracellular calcium sensitivity of transmitter release during synaptic facilitation. *Neuron* **37**, 801–811 (2003).
12. Wu, X. S. & Wu, L. G. Protein kinase C increases the apparent affinity of the release machinery to Ca^{2+} by enhancing the release machinery downstream of the Ca^{2+} sensor. *J. Neurosci.* **21**, 7928–7936 (2001).
13. Ishikawa, T., Sahara, Y. & Takahashi, T. A single packet of transmitter does not saturate postsynaptic glutamate receptors. *Neuron* **34**, 613–621 (2002).
14. Gillis, K. D., Mößner, R. & Neher, E. Protein kinase C enhances exocytosis from chromaffin cells by increasing the size of the readily releasable pool of secretory granules. *Neuron* **16**, 1209–1220 (1996).
15. Stevens, C. F. & Sullivan, J. M. Regulation of the readily releasable vesicle pool by protein kinase C. *Neuron* **21**, 885–893 (1998).
16. Sakaba, T. & Neher, E. Calmodulin mediates rapid recruitment of fast-releasing synaptic vesicles at a calyx-type synapse. *Neuron* **32**, 1119–1131 (2001).
17. Deitcher, D. L. *et al.* Distinct requirements for evoked and spontaneous release of neurotransmitter are revealed by mutations in the *Drosophila* gene *neuronal-synaptobrevin*. *J. Neurosci.* **18**, 2028–2039 (1998).
18. Schoch, S. *et al.* SNARE function analyzed in synaptobrevin/VAMP knockout mice. *Science* **294**, 1117–1122 (2001).
19. Washbourne, P. *et al.* Genetic ablation of the t-SNARE SNAP-25 distinguishes mechanisms of neuroexocytosis. *Nature Neurosci.* **5**, 19–26 (2002).
20. Yang, Y., Udayasankar, S., Dunning, J., Chen, P. & Gillis, K. D. A highly Ca^{2+}-sensitive pool of vesicles is regulated by protein kinase C in adrenal chromaffin cells. *Proc. Natl Acad. Sci. USA* **99**, 17060–17065 (2002).
21. Monod, J., Wyman, J. & Changeux, J.-P. On the nature of allosteric transitions: A plausible model. *J. Mol. Biol.* **12**, 88–118 (1965).
22. Li, J., Zagotta, W. N. & Lester, H. A. Cyclic nucleotide-gated channels: structural basis of ligand efficacy and allosteric modulation. *Q. Rev. Biophys.* **30**, 177–193 (1997).
23. Zhu, H., Hille, B. & Xu, T. Sensitization of regulated exocytosis by protein kinase C. *Proc. Natl Acad. Sci. USA* **99**, 17055–17059 (2002).
24. Stevens, C. F. & Wesseling, J. F. Augmentation is a potentiation of the exocytotic process. *Neuron* **22**, 139–146 (1999).
25. Scanziani, M., Capogna, M., Gähwiler, B. H. & Thompson, S. M. Presynaptic inhibition of miniature excitatory synaptic currents by baclofen and adenosine in the hippocampus. *Neuron* **9**, 919–927 (1992).
26. Piedras-Rentería, E. S. *et al.* Presynaptic homeostasis at CNS nerve terminals compensates for lack of a key Ca^{2+} entry pathway. *Proc. Natl Acad. Sci. USA* **101**, 3609–3614 (2004).
27. Delaney, K. R. & Tank, D. W. A quantitative measurement of the dependence of short-term synaptic enhancement on presynaptic residual calcium. *J. Neurosci.* **14**, 5885–5902 (1994).
28. Angleson, J. K. & Betz, W. J. Intraterminal Ca^{2+} and spontaneous transmitter release at the frog neuromuscular junction. *J. Neurophysiol.* **85**, 287–294 (2001).